

# Optimization of capillary zone electrophoresis–electrospray mass spectrometry for cationic and anionic laser dye analysis employing opposite polarities at the injector and interface

Johnson Varghese and Richard B. Cole\*

*Department of Chemistry, University of New Orleans, Lakefront Campus, New Orleans, LA 70148 (USA)*

(First received November 10th, 1992; revised manuscript received February 11th, 1993)

---

## ABSTRACT

On-line capillary zone electrophoresis–electrospray mass spectrometry (CZE–ES–MS) has been used to investigate the purity of laser dyes. A CZE–ES–MS interface linking a Dionex CE System I and a Vestec 201 electrospray mass spectrometer was constructed and employed for this purpose. Interface optimization studies revealed that maximum sensitivity conditions are significantly different from maximum stability conditions. Use of a cationic surfactant, cetyltrimethylammonium chloride, proved effective at reducing the interaction between the cationic laser dye, Rhodamine 6G, and the wall of the silica capillary, a problem which can otherwise persist even at low pH. To direct electroosmotic flow towards the detector, negative voltages were applied to the CZE source vial. This enabled efficient separation of Rhodamine 6G from low level isomeric and analogue impurities which were detected using positive voltages at the mass spectrometer ion source. Despite intrinsic difficulties associated with negative-ion ES–MS, negative-ion detection was used in combination with positive CZE potentials to separate and characterize analogue impurities found in the anionic laser dye Eosin Y. Impurities present in such laser dyes can have profound effects on the operating efficiencies of dye lasers and the usable lifetime of the dye.

---

## INTRODUCTION

Interest in capillary electrophoresis (CE) from both the research and commercial standpoints has increased dramatically within the last five years. Capillary electrophoresis may be subdivided into several categories including capillary zone electrophoresis (CZE) [1], micellar electrokinetic capillary chromatography (MECC) [2], gel CE [3], isotachopheresis [4] and isoelectric focusing [5]. These techniques can provide separation of closely related structures in a relatively short time period [6] as compared to

conventional liquid separation techniques such as high-performance liquid chromatography [7].

Information regarding the structures of unknown analytes present in sample mixtures can be obtained with highest specificity when a mass spectrometer is used as the detector. Coupling of capillary electrophoresis with mass spectrometry (MS) is aided by the prerequisite of both techniques that analytes be present in ionic form. From a mass spectrometry perspective, CE–MS interfacing has relied upon electrospray (ES) [8], “ion-spray” [9], and fast atom bombardment (FAB) [10,11] ionization techniques which have been adapted to allow efficient on-line transfer of materials eluting from an electrophoretic column into the gas phase. The “spray” ionization techniques, in particular electrospray and ion-spray, have been utilized in the liquid sheath

---

\* Corresponding author.

electrode [8] and the liquid-junction [9] interfaces. These approaches offer the capability to interface a variety of capillary types to mass spectrometers, thus accommodating a wide range of samples.

The challenge of CE–MS interfacing is to maintain proper operating conditions on both sides of the interface, *e.g.*, fixed potentials of sufficient magnitude at the CZE source vial and the electrospray needle to permit reproducible, high-efficiency CE separations, and allow high ion currents at the mass spectrometer. The incorporation of a make-up flow just prior to MS analysis has allowed stable ionization of the column eluent. In the case of electrospray [8] or “ion-spray” [9] techniques, typically methanol and acetonitrile are used, whereas glycerol or other liquid matrix materials are essential in flow-FAB [10,11] experiments.

Olivares *et al.* [12] reported the first successful coupling of CZE and MS. This initial work evolved into the liquid sheath electrode interface [8] where electrical contact is made at the capillary terminus via a steady liquid flow. Proper mixing of the sheath liquid and the CZE eluent allows the use of aqueous buffers of relatively high ionic strength which cannot be used in the absence of sheath flow. The operation of the interface was found to be relatively unaffected by variations in CZE flow-rates. The CZE capillary was placed in the interior of the stainless-steel electrospray needle such that the capillary terminus protruded approximately 0.1 to 0.2 mm, in order to minimize zone broadening. At the needle voltage corresponding to the onset of electrospray, the liquid sheath enables formation of the characteristic “Taylor cone” [13] at the tip of the protruding capillary. This arrangement allows adequate mixing of the CZE eluent and the sheath flow, permitting a stable electrospray current.

This paper describes the in-house construction, optimization, and application of a CZE–MS interface linking two commercially available instruments, *i.e.*, a capillary electrophoresis System I (Dionex, Sunnyvale, CA, USA) and a 201 electrospray mass spectrometer (Vestec, Houston, TX, USA). The combined instrumentation has been used to investigate the

purity of selected cationic and anionic laser dyes. Solutions of such organic dyes are used in laser sources to offer both pulsed and continuous laser operation over a continuum of wavelengths from the near-UV to the near-IR [14]. Such dye lasers not only offer tunability of wavelength, but also a facility in cooling (largely due to the fact that the dyes are present in solution) that permits intense laser pumping at high pulse repetition rates [15]. The purity of such laser dyes can profoundly affect the laser efficiency and the usable lifetime of the dye. Secondary products generated in the manufacture of laser dyes are quite likely to be of inferior efficiency for laser operation. Furthermore, impurities may quench laser activity at variable rates, leading to a deterioration of laser power. For these reasons, assessment of laser dye purity can be of high importance to the large constituency of dye laser users.

## EXPERIMENTAL

### Chemicals

Rhodamine 6G (95% and 99% purity levels) was purchased from Eastman Kodak (Rochester, NY, USA) and Aldrich (St. Louis, MO, USA). Eosin Y (92%) was also purchased from Aldrich, as was cetyltrimethyl ammonium chloride (CTAC). CZE buffers utilized ammonium acetate and ammonium hydroxide from J.T. Baker (Phillipsburg, NJ, USA); sodium chloride was purchased from EM Industries (Gibbstown, NJ, USA). All solvents used (*i.e.*, water and methanol from EM Industries) were HPLC grade.

### Capillary zone electrophoresis

Both CZE–UV and on-line CZE–ES–MS were performed using the Dionex CE System I. For all applications reported, the constant-voltage CE mode was employed. For off-line work, UV–Vis absorbance detection was used. Flexibility was provided by the three modes of sample introduction: electrokinetic, gravity and pressure. Vitreous silica capillaries were employed in all analyses; 50  $\mu\text{m}$  I.D., 220  $\mu\text{m}$  O.D. were purchased from SGE (Austin, TX, USA); 100

$\mu\text{m}$  I.D., 235  $\mu\text{m}$  O.D. from Polymicro (Phoenix, AZ, USA).

### Electrospray mass spectrometry

A Vestec 201 electrospray mass spectrometer was employed for all mass spectral analyses [16]. Collisionally induced dissociations were minimized in all experiments by maintaining a low skimmer–collimator voltage difference. A Sage syringe pump (Orion Research, Boston, MA, USA) was used for direct infusion of solutions during off-line ES-MS work and for the delivery of the sheath flow of liquid during CZE–ES-MS.

### CZE–ES-MS interface

The manufacturer's electrospray probe was replaced by a CZE–ES-MS interface probe constructed in-house at the University of New Orleans (Fig. 1) which allowed for delivery of a "make-up" fluid and an electrical contact at the capillary exit, in an analogous fashion to the sheath flow set-up described previously by Smith *et al.* [8]. In order to introduce the sheath flow (typically 100% methanol at 2.9  $\mu\text{l}/\text{min}$ ), a portion of the CZE capillary (17 cm) was placed inside a stainless-steel capillary via a 1/16 in. (1 in. = 2.54 cm) stainless-steel make-up "tee". To avoid terminology confusion, stainless-steel capillaries used for ES-MS are hereafter referred to as "needles", in order to distinguish them from silica capillaries. The electrospray voltage (+2.45 to 2.85 kV for cation analysis) was applied directly to this tee rather than to the

needle tip. For cation analysis, the counter electrode (nozzle), skimmer and collimator were maintained at 200 to 300 V, 9 to 14 V, and 10 V, respectively. Negative voltages of similar magnitude were used during analyses of anions. The Dionex CE System I was directly coupled to the MS system without additional modifications. The dual polarity power supply can deliver a constant voltage to the source vial (up to  $\pm 30$  kV) with the CZE capillary removed from the destination vial. The CZE source vial was typically maintained between 20 and 25 kV (–20 and –25 kV for reversed-polarity work) while ensuring that the CZE current drawn from the power supply did not exceed 10–15  $\mu\text{A}$ , to maintain electrospray stability. Cleaning (with 0.1 M NaOH) and filling of the capillaries (with fresh buffers) were made easy by the pressure inject facility on the CE instrument. The problem of continuous siphoning during sample introduction or CZE operation was avoided by maintaining the source buffer and the capillary exit at approximately the same levels.

### RESULTS AND DISCUSSION

#### Construction of the liquid sheath electrode interface

The liquid sheath flow [8] type CZE–MS coupling was chosen for the Vestec electrospray mass spectrometer mainly due to design and positioning constraints of the electrospray chamber. The theory of CZE, as first described by Jorgenson and Luckacs [1], proposes that column efficiencies are not dependent upon capillary length. Rapid, high-resolution separations are thus possible using rather short capillaries. Since the electrospray source has a 16.5 cm probe shaft leading to the nozzle (counter electrode), the terminal end of the CZE–sheath flow system had to be fitted with a retractable probe of this length (Fig. 1) which was constructed in-house at the University of New Orleans. The probe dimensions and the physical geometry of the CZE instrument necessitated the use of capillaries of at least 100 cm in length for on-line CZE–MS analysis. Although non-ideal for CZE purposes, the use of longer capillaries reduced the problem of voltage fluctu-

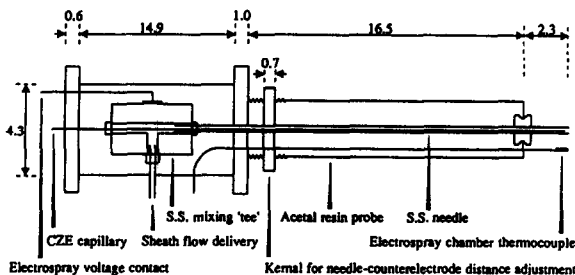


Fig. 1. Schematic diagram of the interface constructed to couple the Dionex CE System I to the Vestec 201 electrospray mass spectrometer. All dimensions are given in centimetres. For all applications reported, the CZE capillary tip was held (ca. 1.0 mm) inside the stainless-steel (S.S.) needle. During operation the platform supporting the tee is covered by a plexiglass case for safety purposes.

tuations at the electrospray needle because of the greater resistance between the CZE source vial and the ES-MS needle.

#### Optimization of the CZE–MS interface

Placement of the CZE silica capillary relative to the ES needle has a large effect on ES-MS signal characteristics. Smith *et al.* [8] reported that when the exit of the CZE capillary was pulled back inside of the stainless-steel needle tip, a loss of analyte signal resulted, possibly due to electrochemical processes taking place on the metallic needle surface. In order to systematically investigate the manner in which electrospray signals are affected by changes in the CZE capillary size and position within a given stainless-steel needle, two CZE capillaries (50 and 100  $\mu\text{m}$  I.D.; both 220 to 235  $\mu\text{m}$  O.D.) were tested in conjunction with three different needle sizes (250, 300, and 350  $\mu\text{m}$  I.D.; all 500  $\mu\text{m}$  O.D.). For each combination of stainless-steel needle and silica capillary, several arrangements were adopted: silica capillary tip approximately 1 mm inside the needle, silica capillary tip adjacent with the stainless-steel needle exit, and silica capillary tip approximately 0.2 mm outside the stainless-steel needle exit.

Rhodamine 6G, the most widely used laser dye in the world as of 1990 [14], was selected as the test compound. A 100  $\text{ng}/\mu\text{l}$  solution was electroosmotically infused through the vitreous silica capillary, and a sheath flow of methanol (100%) was introduced at a flow-rate of 2.9  $\mu\text{l}/\text{min}$ . Application of CZE voltage initiated electroosmotic flow and movement of Rhodamine 6G towards the detector end. Electrospray parameters were optimized to obtain the maximum stable current for the “parent” cation ( $m/z$  443). Successful mixing of the CZE eluent and sheath flow, hence, the establishment of a stable potential gradient along the capillary, was verified by monitoring the electrospray current measured at the nozzle. At the onset of CZE voltage the electrospray current was observed to increase.

Plots of  $m/z$  443 ion current at the detector vs. capillary position appear in Fig. 2. Each data point represents the integrated ion current obtained over 118 s. Data for the 100  $\mu\text{m}$  and 50

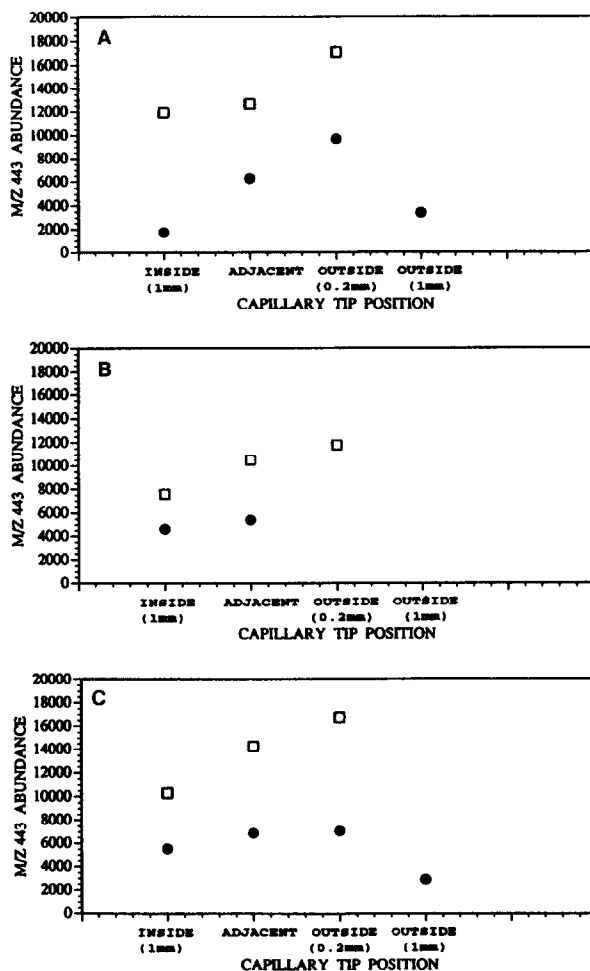


Fig. 2. Plots of  $m/z$  443 abundance from Rhodamine 6G vs. CZE capillary tip position relative to the fixed stainless-steel needle having an I.D. of: (A) 250  $\mu\text{m}$ , (B) 300  $\mu\text{m}$ , and (C) 350  $\mu\text{m}$ . The laser dye (100  $\text{ng}/\mu\text{l}$ ) was electroosmotically infused ( $-20$  kV) through vitreous silica capillaries [50  $\mu\text{m}$  ( $\bullet$ ) and 100  $\mu\text{m}$  ( $\square$ ) I.D., both 100 cm in length] in the presence of cetyltrimethylammonium chloride.

$\mu\text{m}$  I.D. silica capillaries were acquired on consecutive days. For a particular capillary and stainless-steel needle size, data for the various capillary positions were acquired in rapid sequence. This procedure was repeated at the next needle size. The use of unconventionally large I.D. electrospray needles was necessitated by the requirement of “housing” fused-silica capillaries having O.D.s near 240  $\mu\text{m}$ . Blockage of the silica capillary prevented the acquisition of the final data points for the 300  $\mu\text{m}$  I.D. stainless-

steel needle in combination with the 50  $\mu\text{m}$  I.D. capillary.

From Fig. 2, certain conclusions can be drawn regarding the stability and ease of generating high ES-MS signals. In all cases, the higher throughput of the larger (100  $\mu\text{m}$ ) silica capillary resulted in a higher  $m/z$  443 ion current. Furthermore, for all the needles tested, as the silica tip was moved from inside the stainless-steel needle to outside, the ion current at the detector was observed to increase. When the tip extended beyond the needle by 0.1 to 0.2 mm, optimum sensitivity was obtained. At more extreme extensions (e.g., 1 mm outside, for the 50  $\mu\text{m}$  I.D. capillaries in combination with 250 or 350  $\mu\text{m}$  needles, Fig. 2), signal intensity was observed to decrease.

The initial increase in ion current observed when the silica capillary begins to protrude from the stainless-steel needle can be attributed to a decrease in mixing volume leading to less dilution by the sheath liquid. Furthermore, with the silica protruding slightly, it is likely that finer droplets will be formed via the electrospray process, leading to more efficient ion production, as compared to the case where electrospray occurs directly from the tip of a wide-bore needle. Beyond a certain point, however, the silica tip protrudes too far to enable adequate mixing.

Although optimum sensitivities could be obtained with the tip protruding 0.1 to 0.2 mm outside the capillary, certain disadvantages existed for this configuration. When the CZE buffer exceeded a critical concentration, conductance down the CZE capillary created excess charging at the electrospray needle tip, resulting in inherent instability and a tendency toward electric discharge. This effect became more pronounced as the silica capillary was moved further outside the stainless-steel needle or when larger I.D. capillaries were used. In addition, after approximately one hour of constant operation, the silica tip invariably experienced deterioration causing loss of signal and necessitating removal of the affected region of the capillary. In coupling a CZE system to a Vestec electrospray source, Parker *et al.* [17] used silica capillaries having larger outer diameters (360

$\mu\text{m}$  O.D., 75  $\mu\text{m}$  I.D.) than those used in this investigation. This necessitated the use of wide-diameter stainless-steel needles (700  $\mu\text{m}$  O.D., 425  $\mu\text{m}$  I.D.) to house the large-diameter capillaries and provide a make-up flow. In their setup, the silica tip was always placed outside of the stainless-steel needle and degradation of the silica was not observed, presumably due to the greater material thickness of the larger silica capillaries.

In order to characterize the relationship between CZE voltage and generated electrospray current, a capillary (100  $\mu\text{m}$  I.D., total length 100 cm) filled with an electrolyte (5 mM NaCl) was placed in a 300  $\mu\text{m}$  I.D. stainless-steel needle. A series of voltages (0 to 30 kV) was then applied to the anodic (source) reservoir also containing the electrolyte. As before, a sheath flow of methanol (100%) was introduced at the interface. Using a constant electrospray voltage, the total ion current (measured at the nozzle) due purely to liquid sheath flow was recorded. The CZE voltage was then increased by increments of 4 kV while the generated electrospray currents were recorded. The complete operation was repeated using three different silica capillary tip positions (1 mm inside, adjacent, and 0.2 mm outside, relative to the stainless-steel needle); findings are plotted in Fig. 3. This figure shows that regardless of capillary tip position, electrospray current increases with CZE voltage. Optimal operating conditions of the electrospray mass spectrometer, however, necessitate a low contribution to electrospray current from corona discharge processes [18,19]. The manufacturer recommends that current at the counter electrode should be maintained below 250 nA, to avoid electric discharge conditions. One can conclude that placement of the capillary tip inside the stainless-steel needle allows operation at higher CZE voltages before discharge conditions are reached. Of course the electrospray needle voltage can be lowered somewhat to alleviate the electric discharge problem, but this often has adverse effects upon electrospray sensitivity and stability.

Despite some loss in ultimate sensitivity, placement of the capillary inside the needle afforded ruggedness to the interface, hence, this

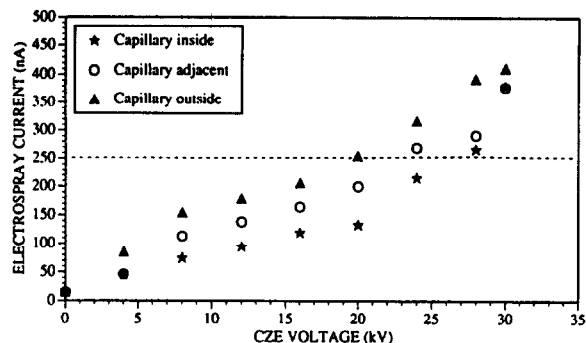


Fig. 3. Plot of total electrospray current (measured at the "nozzle" counterelectrode) as a function of applied CZE voltage for a CZE-MS interface employing a 300  $\mu\text{m}$  I.D. stainless-steel needle with a 100  $\mu\text{m}$  I.D. silica column whose exit tip was placed within (*ca.* 1 mm), adjacent to, and outside (0.2 mm) the needle. Aqueous NaCl (5 mM) was employed as the buffer with a sheath flow (2.9  $\mu\text{l}/\text{min}$ ) of methanol (100%). The dashed line signifies the manufacturer's suggested current limit at the counterelectrode, such that electric discharge processes are minor.

configuration was adopted for analyses where sensitivity was not the limiting issue. Under these conditions, fluctuations in the applied voltages or variation in buffer properties (including uneven liquid sheath flow-rates) did not degrade electrical contact at the interface. Furthermore, long periods of analysis were possible with no loss in stability. Although dilution of the buffer and the potential for zone broadening are greater with the silica capillary inside, the ability to use high ionic strength buffers (*e.g.*, 10 mM) is improved (electrospray stability is maintained). Presumably the current due to capillary conductance is dissipated more efficiently when the silica capillary is within the stainless-steel needle.

#### Normal-polarity CZE-MS of Rhodamine 6G

Displayed in Fig. 4 is the ES-MS spectrum (parent ion region only) of Rhodamine 6G, obtained by electroosmotically infusing a 100 ng/ $\mu\text{l}$  solution through the CZE-ES-MS interface. The Rhodamine 6G cation (structure shown in Fig. 4) appears at  $m/z$  443; in addition, under minimal fragmentation conditions, ions were also noted at  $m/z$  415. In ex-

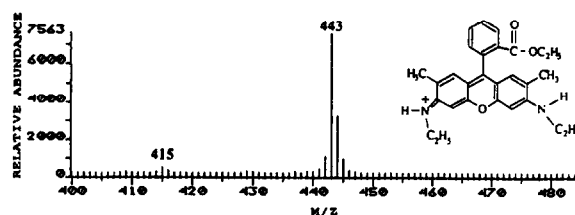


Fig. 4. Electrospray mass spectrum of Rhodamine 6G in the presence of cetyltrimethylammonium chloride, obtained by electroosmotic infusion employing CZE and MS conditions typically used during on-line CZE-ES-MS (see Fig. 6).

aming Rhodamine 6G of various grades available from different manufacturers, it became clear that contaminants were prevalent even among "high-purity" products. From direct MS measurements alone, it is not possible to evaluate whether isomeric impurities are present, hence, the development of on-line CE-MS methodology was pursued to clarify the purity issue.

A common problem encountered in CZE analysis is that of adsorption of cationic molecules (*e.g.*, polypeptides [20]) onto the wall of the fused-silica capillary. An attempt was made to reduce this effect by employing acetic acid (1% glacial, pH 2.9) to selectively protonate fixed anionic sites on the capillary. However, direct CZE using this approach (Fig. 5a) was found to be unsuccessful due to a failure to achieve complete wall deactivation. Although wall adsorption is an anticipated problem when switching to a borate buffer (pH adjusted to alkaline), peak tailing can be alleviated by the presence of electroosmotic flow. Despite significant tailing, in addition to the main component at  $m/z$  443 (peak 1, Fig. 5b), the selected-ion electropherogram reveals that a second  $m/z$  443 component (peak 2, presumably an isomer of the main component, Fig. 5b) appeared in four scans. It is possible that the shape of peak 2 was narrowed by the presence of other cationic species in the sample solution, *i.e.*, those comprising the tailing portion of the major peak. Operation at pH 8.9, of course, did not permit deactivation of anionic sites on the silica capillary, hence, alternative buffer systems were investigated.

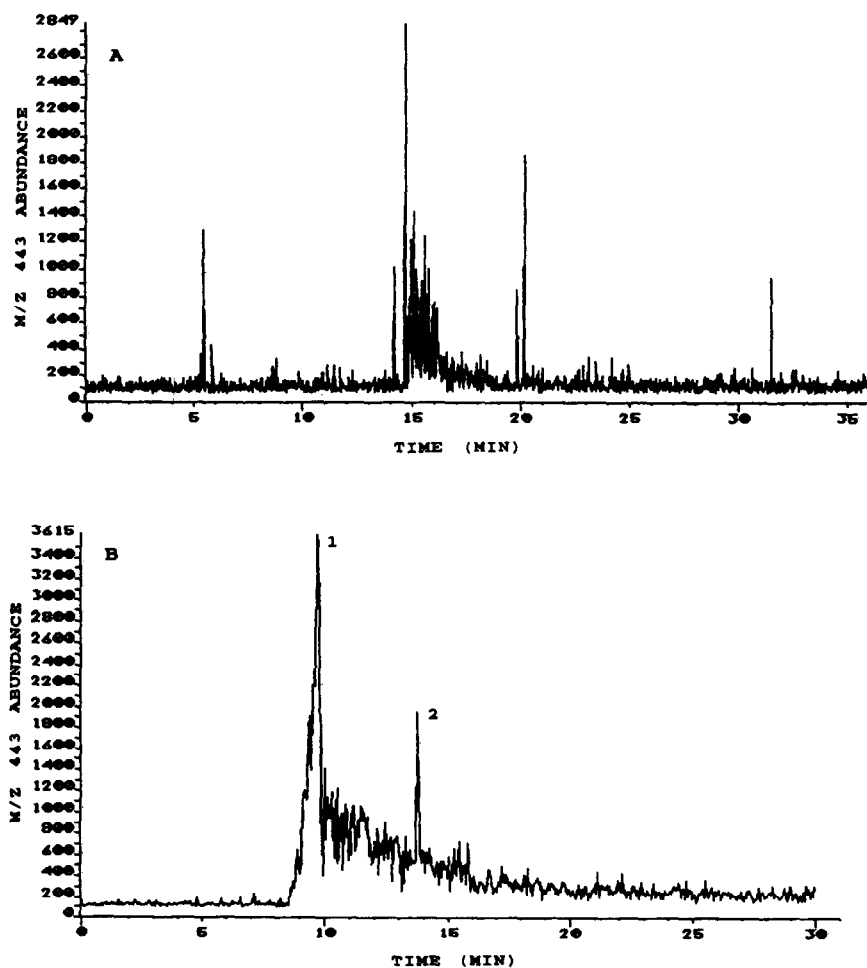


Fig. 5. Selected-ion electropherogram ( $m/z$  443) from the CZE–ES–MS analysis of Rhodamine 6G (100 ng/ $\mu$ l), employing: (A) buffer: glacial acetic acid (1%, v/v), pH 2.9; capillary: 50  $\mu$ m I.D., 220  $\mu$ m O.D., 100 cm in length; sample injection: 10 kV/10 s; CZE voltage: 25 kV; ES voltage: 2.44 kV; MS scan rate: 1.16 s/scan ( $m/z$  100 to 500). (B) Conditions as for (A) except, buffer: sodium borate (10 mM), pH 8.9; MS scan rate: 3.03 s/scan ( $m/z$  100 to 600). Both electropherograms display raw data.

### Reversed-polarity CZE–ES–MS of Rhodamine 6G

Minimization of the interaction between cationic analytes and the silica wall is best achieved by chemically deactivating fixed anionic sites on the wall, or by creating a positively charged layer on the inner surface of the wall. However, electroosmotic flow towards the detector is only possible if CZE is performed in the reversed-polarity mode [21] (negative polarity at the source vial). Recently, the utilization of aminopropyl-silylated (APS) fused-silica capillaries for on-line CZE–MS analysis has been

reported by Mosely and co-workers [22,23]. In that reversed-polarity work, with the bonded phase positively charged at or below pH 3.4 (corresponding to the  $pK_a$  value of APS), the electroosmotic flow was reversed in direction and increased in velocity relative to normal-polarity fused-silica capillaries. Efficient peptide separations were reported utilizing these columns in conjunction with low pH buffers and a coaxial interface.

Other studies have shown that certain electrolytes can alter the rate of electroosmotic flow and even reverse the direction of flow in fused-

silica capillaries. In particular, quaternary ammonium surfactants have been shown to be effective in this regard. Terabe *et al.* [21] first reported the utilization of cetyltrimethylammonium bromide (CTAB) to reverse electroosmotic flow via formation of a positively charged layer on the inner surface of the silica capillary. Altria and Simpson [24] showed that under equivalent conditions, an increase in flow-rate by one order of magnitude occurred for capillaries filled with CTAB (2 mM) as compared to bare silica capillaries containing phosphate buffers (2 mM). A homologue of CTAB, tetradecyltrimethylammonium bromide (TTAB), was also used by Huang *et al.* [25] to separate a series of low-molecular mass carboxylic acids. Again, reversed-polarity conditions were employed allowing separation of six acids within 3.5 min. In that study, reversal of flow was initiated at a minimum TTAB concentration of 0.4 mM.

In an effort to improve upon electropherograms shown in Fig. 5, the cationic surfactant, cetyltrimethylammonium chloride (CTAC) was added to the CZE buffer (0.5 mM). Selected-ion

electropherograms for the analysis of a solution of Rhodamine 6G (100 ng/ $\mu$ l), corresponding to 6.41 pmol loaded on column, appear in Fig. 6. The mass spectrometer was scanned from  $m/z$  442 to 445. Close inspection of the “blow-up” of the  $m/z$  443 electropherogram (inset in Fig. 6) reveals that a minimum of three, maybe four, peaks were present in addition to the main component. These impurities were estimated to represent approximately 3 to 4% of the total observed ion current. Most likely, these later eluting peaks correspond to isomers of Rhodamine 6G. To improve the signal-to-noise ratio for the minor components, the concentration of Rhodamine 6G was increased by a factor of ten (to 1  $\mu$ g/ $\mu$ l, representing 64.1 pmol on column). The analysis was repeated under the same conditions, except that the mass spectrometer was scanned over a larger range (from  $m/z$  300 to 600) in order to detect other (non-isomeric) contaminants. “Overloading” of the column for the main component, resulted in a baseline width of 1 min (Fig. 7, top), compared to 20 s for the more dilute sample (Fig. 6).

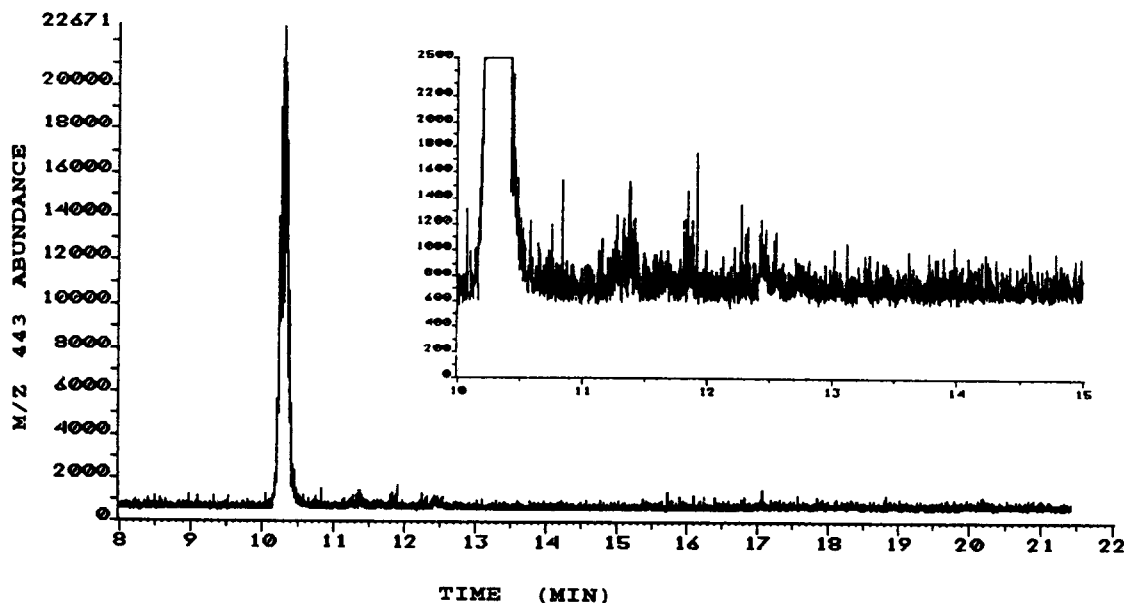


Fig. 6. Selected-ion electropherogram ( $m/z$  443) showing raw data from the CZE-ES-MS analysis of Rhodamine 6G (100 ng/ $\mu$ l solution/6.41 pmoles on column). Buffer: CTAC (0.5 mM) and NaCl (5 mM), pH 6.2; capillary: 100  $\mu$ m I.D.; 235  $\mu$ m O.D.; 100 cm in length; sample injection: 100 mm/10 s; CZE voltage: 20 kV; ES voltage: 2.8 kV; MS scan rate: 0.07 s/scan ( $m/z$  442 to 445). Inset shows magnified view of response between 10 and 15 min.



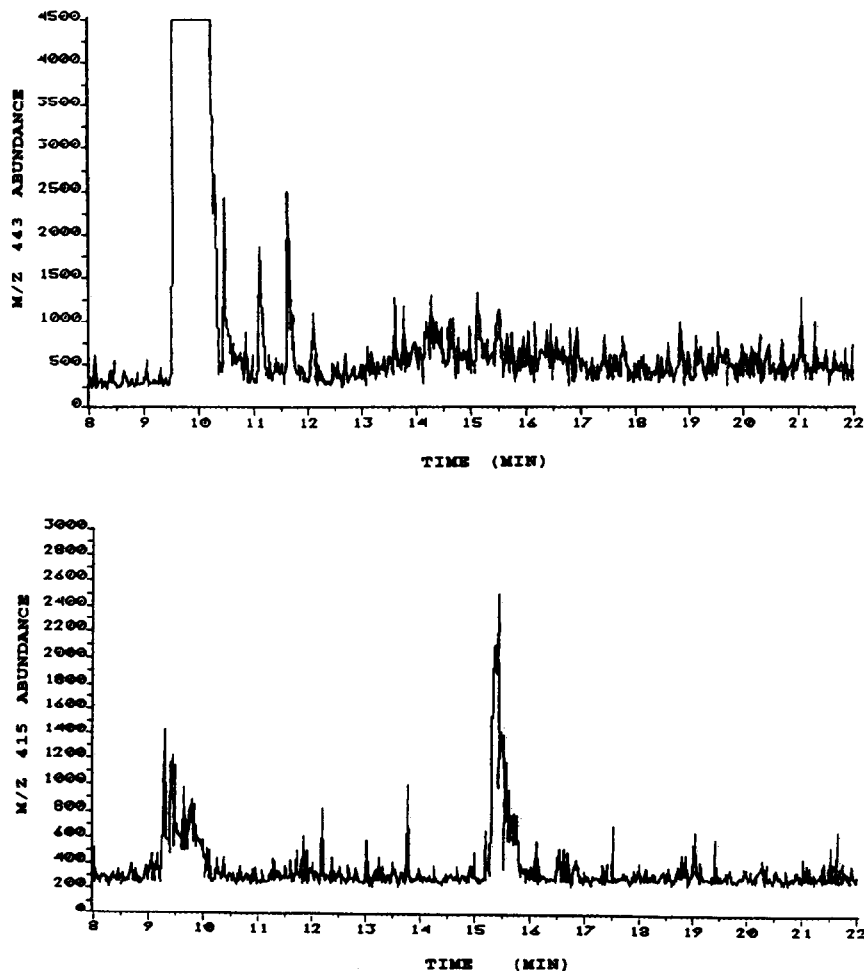


Fig. 7. Selected-ion electropherograms of  $m/z$  443 (top) and  $m/z$  415 (bottom) from the CZE-ES-MS analysis of Rhodamine 6G. Conditions as for Fig. 6, except concentration of Rhodamine 6G is now 1000 ng/ $\mu$ l (64.1 pmoles on column) and MS scan rate is 1.21 s/scan ( $m/z$  300 to 600). Both electropherograms display raw data.

However, this exercise did have the desired effect of pulling the minor peaks out of the noise background. Four definite, reproducible peaks consisting of several (1.2 s) mass spectrometer scans each, clearly appear between 10.5 and 12.5 min.

The increase in sample concentration and scan range also enabled detection of peaks at  $m/z$  415 which have heights similar to the  $m/z$  443 impurities. Two components at  $m/z$  415, separated by approximately 6 min appeared in the electropherogram (Fig. 7, bottom) of Rhodamine 6G purchased from one manufacturer. Other Rhodamine 6G from different manufac-

turers showed only one impurity at  $m/z$  415, eluting at approximately 15.5 min. It is plausible that the early eluting  $m/z$  415 impurity corresponds to a hydrolyzed form of Rhodamine 6G, where the ethyl ester has been converted to a carboxylic acid. Appearance of the carboxylate anion (zwitterionic) form could cause the  $m/z$  415 peak to elute in front of Rhodamine 6G, as was indeed observed in Fig. 7. The empirical formula of the later eluting  $m/z$  415 impurity is also likely to be the same as that of Rhodamine 6G less  $C_2H_4$ ; this may arise via deficiency of an ethyl substituent (replaced by a hydrogen atom) at either nitrogen site.

The high level of reproducibility of all data with minor variations in retention times, and the evidence of adequate separations were sufficient to validate the analysis. Rhodamine 6G must be prepared in solutions containing the same concentration of CTAC as the buffer. This insures that the silica sites will retain positively charged cetyltrimethylammonium cations, thus minimizing adsorption of analyte onto the capillary walls. It should be noted that a large bulk flow of any reagent into the ES ion source will often degrade sensitivity for analytes. Furthermore, adsorption of reagents onto the nozzle and other electrospray source components contribute to the degradation of all signals at the MS detector, necessitating cleaning of the ES counter electrode after each full day of use. The CTAC cation has a molecular mass of 284. Under the employed conditions, the abundance of  $m/z$  284 ions is high enough to saturate the detector, thus, MS scanning over this background peak was avoided.

#### Normal-polarity CZE-ES-MS of Eosin Y

Certain commercially important laser dyes such as Eosin Y contain anionic functional groups, hence, ES-MS in the negative ion mode can best be used to optimize detection of impurities which may be present. On-line normal-mode CZE-negative ion-MS has already been applied to the analysis of negatively charged species using a liquid-junction interface [26]. The physical gap of 10 to 20  $\mu\text{m}$  which comprises the liquid junction effectively decoupled the CZE from the MS and allowed the use of a positive voltage at the CZE source vial and a negative voltage at the electrospray needle.

CZE-UV analysis revealed the reproducible presence of two major components of the Eosin Y laser dye (Fig. 8). Off-line negative-ion ES-MS (Fig. 9) offered more information concerning the composition of the mixture. In the mass spectrum, singly charged ( $m/z$  647) and doubly charged ( $m/z$  323) species representative of Eosin Y were apparent (Fig. 9A and B, respectively). A clear isotope distribution pattern reveals the presence of four bromines in both the singly and doubly charged species. Also present in the low fragmentation mass spectrum of Eosin

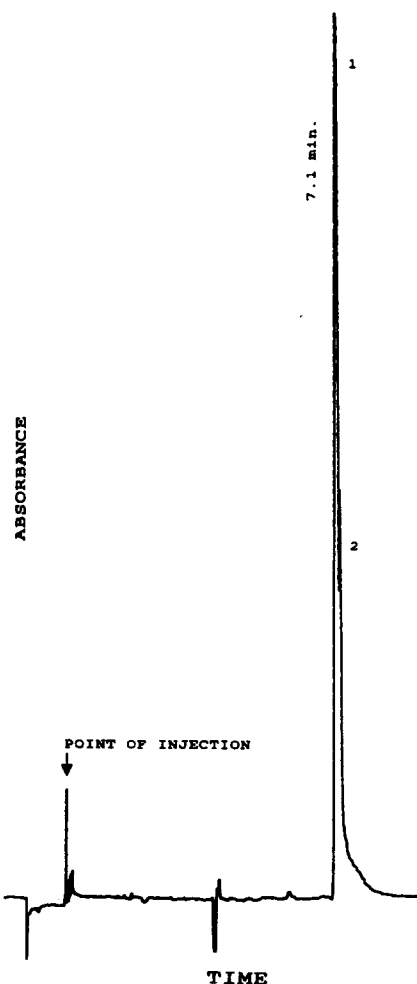


Fig. 8. CZE-UV trace displaying the presence of two components in Eosin Y (100 ng/ $\mu\text{l}$ ). Column: 75  $\mu\text{m}$  I.D., 65 cm in length; buffer: sodium borate (5 mM), pH 9.05; sample injection: 100 mm/7 s; CZE voltage: 25 kV; detection: 254 nm.

Y were ions yielding an isotope distribution pattern characteristic of an impurity containing three bromine atoms. These signals appeared at  $m/z$  567 and  $m/z$  283 (Fig. 9C and D) corresponding to singly and doubly charged molecules, respectively.

In developing a normal-polarity CZE method to analyze negatively charged compounds, the use of normal bare silica columns is highly suited for creating a satisfactory electroosmotic flow and allowing minimal wall interaction. This arrangement again demands the use of opposite

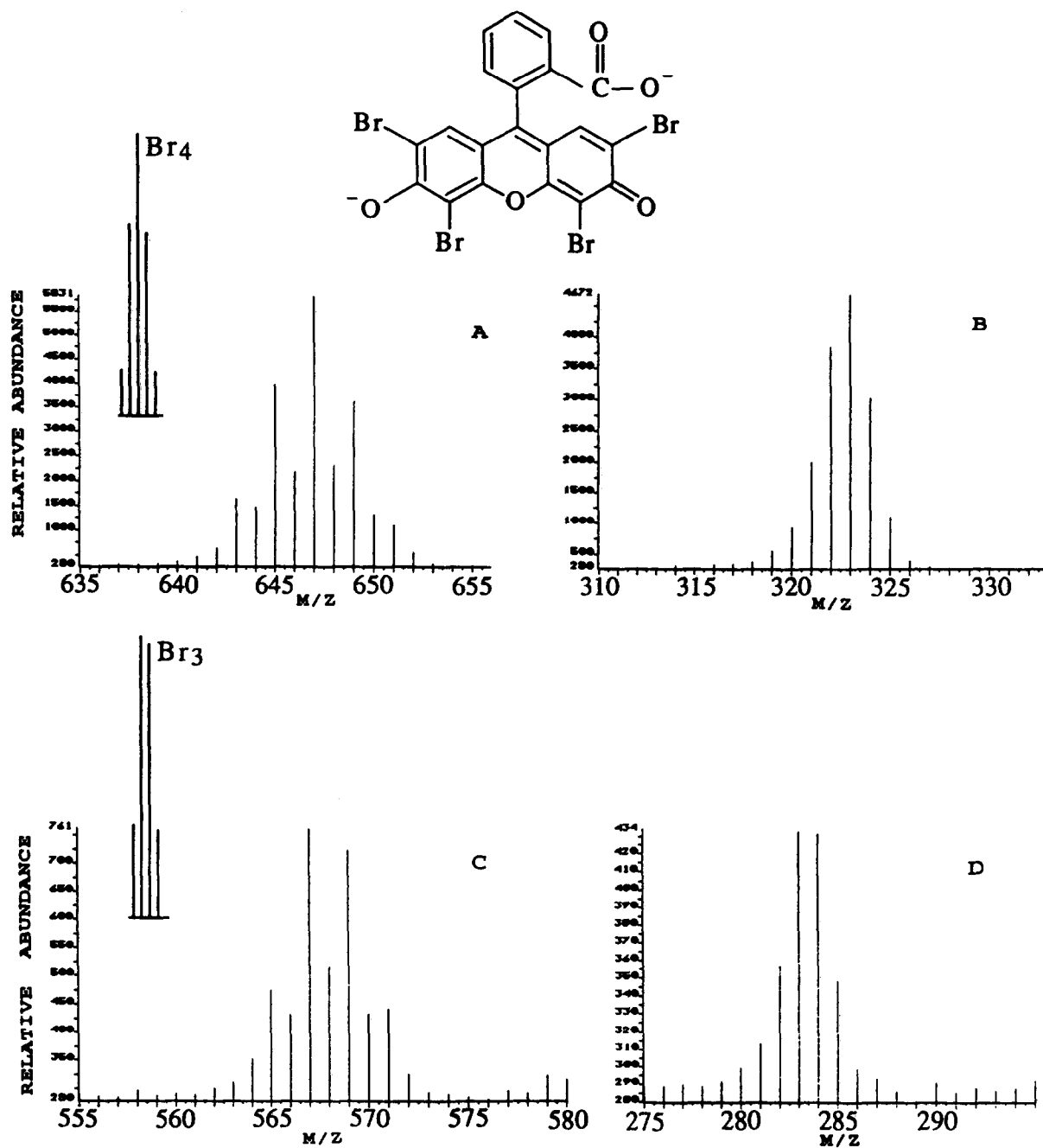


Fig. 9. Negative-ion electrospray mass spectrum of 100 ng/ $\mu$ l Eosin Y (dianion  $M_r = 646$ ) sample generated by direct infusion. (A) Singly charged Eosin Y wherein one anionic site has been protonated. (Inset shows the natural isotopic distribution pattern for a compound containing four bromine atoms [28].) (B) Doubly charged Eosin Y. (C) Singly charged impurity of Eosin Y. (Inset shows the natural isotopic distribution pattern for a compound containing three bromine atoms [28].) (D) Doubly charged impurity of Eosin Y.

polarities for CZE separation (positive) and electrospray ionization (negative). Even with direct infusion of sample, negative-ion electrospray mass spectrometry of aqueous solutions can be wrought with instability problems created by a high tendency toward electric discharge. The corona discharge problem is most severe in the negative-ion mode because electrons can emanate from the edges of the stainless-steel needle held at high negative potentials [19]. Stability of operation at each juncture, of course, is crucial to the success of CZE-MS. The electrical contact established between the source vial at positive potential and the electrospray needle at

negative potential during sheath flow CZE-MS can aggravate an already tenuous situation.

Employing the same type of silica capillary (100  $\mu\text{m}$  I.D.) as for the Rhodamine 6G application, no signals were observed for Eosin Y when electroosmotic infusion of the compound was conducted. This situation was found to be independent of the position of the silica capillary tip in the electrospray needle. Apparently, conductance in the capillary was too great to permit the electrospray needle to sustain a stable negative voltage. Since the capillary was already 100 cm long, increasing the capillary length would lead to unacceptably long analysis times. The

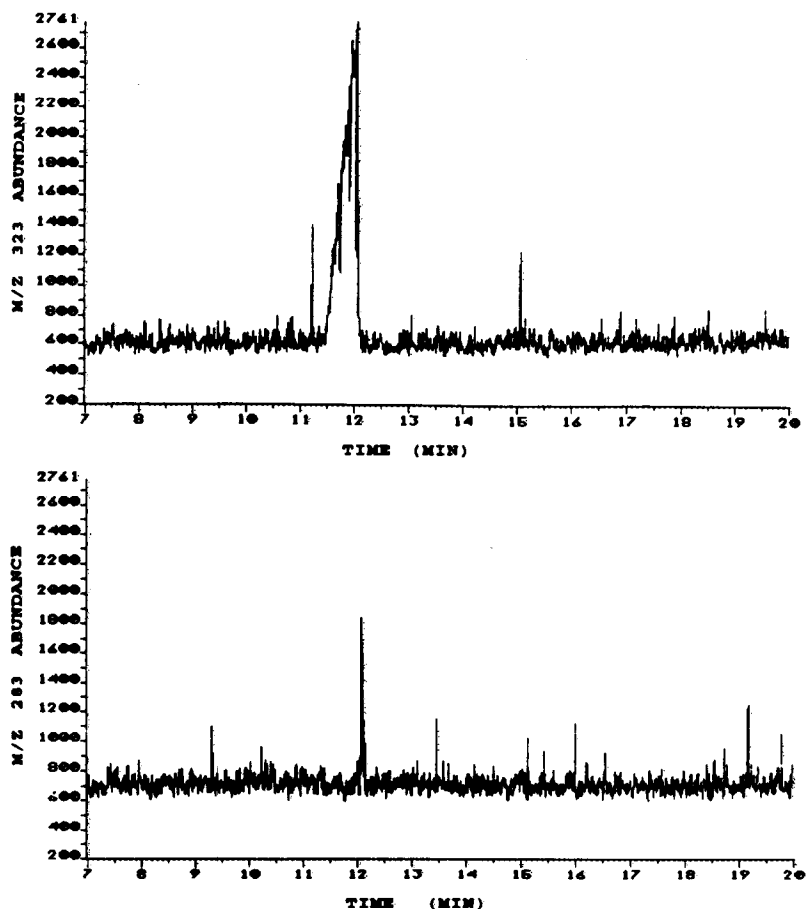


Fig. 10. Single-ion monitoring electropherograms of  $m/z$  323 (top) and  $m/z$  283 (bottom) from 600  $\text{ng}/\mu\text{l}$  Eosin Y sample. Buffer: ammonium acetate (5  $\text{mM}$ ) and ammonium hydroxide (1%, v/v), pH 10.3; capillary: 50  $\mu\text{m}$  I.D., 220  $\mu\text{m}$  O.D., 100 cm in length; sample injection: 10 kV/10 s; CZE voltage: 20 kV; ES voltage: 2.75 kV; MS scan speed: 0.12 s/scan. The data in this figure only have been taken through a "de-spiking" routine.

concentration of the buffer was already too low (5 mM) to consider dilution.

The most effective and practical option to increase the resistance between the two operating voltages was via reduction of the capillary I.D. The utilization of a 50  $\mu\text{m}$  I.D. capillary instead of the 100  $\mu\text{m}$  I.D. capillary (same length) added considerable stability to the negative-ion electrospray current. As was done for Rhodamine 6G, the capillary exit was placed within the electrospray needle to allow greater mixing with the sheath liquid. After examining various buffers, an ammonium acetate–ammonium hydroxide combination was found to be the best suited volatile alkaline buffer (pH 10.3). Under the conditions employed, formation of doubly charged ions occurred in preference to singly charged ions. In the single-ion monitoring (SIM) mode, signals corresponding to the four species viewed in Fig. 9 were acquired as functions of time.

The SIM electropherograms for the doubly charged ions ( $m/z$  323 and 283) are displayed in Fig. 10. Although the electrophoretic peak shape for the  $m/z$  323 ion was poor, separation of the two components was achieved with near baseline resolution. The peak shape for  $m/z$  283 was much better due to a combination of factors. Since this peak corresponds to a minor sample component in the mixture, overloading was avoided. Secondly, as expected, the smaller molecule eluted after the major zone, hence, fronting of the zone was avoided due to the mobility effects of the preceding zone. Fronting of the first zone was probably due to an incompatibility of the buffer wherein the mobility of the analyte was too high in comparison to the mobility of the carrier [27].

The reproducibility of the on-line analysis was found to be quite satisfactory, including the peak distortion for the main zone. Alternative buffers, e.g., sodium borate, were found to be unsuccessful in improving the shape of the main zone. Nevertheless, the separation was adequate to distinguish the two components (their different peak shape was further evidence of heterogeneity). Normal-polarity CZE with negative ion ESM detection thus allowed confirmation of the

presence of an analogous compound containing three bromine atoms as the main impurity in Eosin Y, where the fourth bromine atom has been replaced by a hydrogen atom.

#### ACKNOWLEDGEMENTS

The authors thank Dionex Corporation for providing CE instrumentation for this project. We also thank Drs. Joseph H. Boyer and Piotr Piotrowiak for sharing with us their expertise on the subject of laser dyes. Research funding from the Louisiana Education Quality Support Fund [grant No. (1991–93)-RD-B-15] is gratefully acknowledged.

#### REFERENCES

- 1 J.W. Jorgenson and K.D. Luckacs, *Anal. Chem.*, 53 (1981) 1298.
- 2 S. Terabe, K. Otsuka and T. Ando, *Anal. Chem.*, 57 (1985) 834.
- 3 A.S. Cohen and B.L. Karger, *J. Chromatogr.*, 397 (1987) 409.
- 4 P. Bocek, M. Deml, B. Kaplanova and J. Janak, *J. Chromatogr.*, 160 (1978) 1.
- 5 S. Hjerten and M.D. Zhu, *J. Chromatogr.*, 346 (1985) 265.
- 6 C.A. Monnig and J.W. Jorgenson, *Anal. Chem.*, 63 (1991) 802.
- 7 I.J. Haleem, G.M. Janini, I.Z. Atamna and G.M. Muschik, *J. Liq. Chromatogr.*, 14 (1991) 817.
- 8 R.D. Smith, C.J. Barinaga and H.R. Udseth, *Anal. Chem.*, 60 (1988) 1948.
- 9 E.D. Lee, W. Muck, J.D. Henion and T.R. Covey, *Biomed. Environ. Mass Spectrom.*, 18 (1989) 844.
- 10 R.M. Caprioli, W.T. Moore, M. Martin and B.B. DaGue, *J. Chromatogr.*, 480 (1989) 247.
- 11 M.A. Moseley, L.J. Deterding, K.B. Tomer and J.W. Jorgenson, *Rapid. Commun. Mass Spectrom.*, 3 (1989) 87.
- 12 J.A. Olivares, N.T. Nguyen, C.R. Yonker and R.D. Smith, *Anal. Chem.*, 59 (1987) 1232.
- 13 G.I. Taylor, *Proc. R. Soc. London A*, 280 (1964) 383.
- 14 F.J. Duarte and L.W. Hillman (Editors), *Dye Laser Principles With Applications*, Academic Press, Boston, 1990.
- 15 F.J. Duarte and J.A. Piper, *Appl. Opt.*, 23 (1984) 1391.
- 16 M.H. Allen and M.L. Vestal, *J. Am. Soc. Mass Spectrom.*, 3 (1992) 18.
- 17 C.E. Parker, J.R. Perkins, K.B. Tomer, Y. Shida, K. O'Hara and M. Kono, *J. Am. Soc. Mass Spectrom.*, 3 (1992) 563.

- 18 M.G. Ikonomou, A.T. Blades and P. Kebarle, *J. Am. Soc. Mass Spectrom.*, 2 (1991) 497.
- 19 R.B. Cole and A.K. Harrata, *Rapid Commun. Mass Spectrom.*, 6 (1992) 536.
- 20 J.W. Jorgenson and K.D. Lukacs, *Science*, 222 (1983) 266.
- 21 S. Terabe, K. Ishikawa, K. Utsuka, A. Tsuchiya and T. Ando, *Proceedings of the 26th International Liquid Chromatography Symposium, Kyoto, Japan, Jan., 25–26, 1983*.
- 22 M.A. Moseley, L.J. Deterding, K.B. Tomer and J.W. Jorgenson, *Anal. Chem.*, 63 (1991) 109.
- 23 M.A. Moseley, J.W. Jorgenson, J. Shabanowitz, D.F. Hunt and K.B. Tomer, *J. Am. Soc. Mass Spectrom.*, 3 (1992) 289.
- 24 K.D. Altria and C.F. Simpson, *Anal. Proc. (London)*, 23 (1986) 453.
- 25 X. Huang, J.A. Luckey, M.J. Gordon and R.N. Zare, *Anal. Chem.*, 61 (1989) 766.
- 26 E.D. Lee, W. Muck, J.D. Henion and T.R. Covey, *Biomed. Environ. Mass Spectrom.*, 18 (1989) 253.
- 27 W. Thormann, *Electrophoresis*, 4 (1983) 383.
- 28 F.W. McLafferty, *Interpretation of Mass Spectra*, University Science Books, Mill Valley, CA, 3rd Ed., 1980.